

Discovery of *N*-(2-Chloro-6-methylphenyl)-2-(6-(4-(2-hydroxyethyl)piperazin-1-yl)-2-methylpyrimidin-4-ylamino)thiazole-5-carboxamide (BMS-354825), a Dual Src/Abl Kinase Inhibitor with Potent Antitumor Activity in Preclinical Assays

Louis J. Lombardo,* Francis Y. Lee, Ping Chen, Derek Norris, Joel C. Barrish, Kamelia Behnia, Stephen Castaneda, Lyndon A. M. Cornelius, Jagabandhu Das, Arthur M. Doweyko, Craig Fairchild, John T. Hunt, Ivan Inigo, Kathy Johnston, Amrita Kamath, David Kan, Herbert Klei, Punit Marathe, Suhong Pang, Russell Peterson, Sidney Pitt, Gary L. Schieven, Robert J. Schmidt, John Tokarski, Mei-Li Wen, John Wityak, and Robert M. Borzilleri

Bristol-Myers Squibb Pharmaceutical Research Institute,
P.O. Box 4000, Princeton, New Jersey 08543-4000

Received June 29, 2004

Abstract: A series of substituted 2-(aminopyridyl)- and 2-(aminopyrimidinyl)thiazole-5-carboxamides was identified as potent Src/Abl kinase inhibitors with excellent antiproliferative activity against hematological and solid tumor cell lines. Compound **13** was orally active in a K562 xenograft model of chronic myelogenous leukemia (CML), demonstrating complete tumor regressions and low toxicity at multiple dose levels. On the basis of its robust *in vivo* activity and favorable pharmacokinetic profile, **13** was selected for additional characterization for oncology indications.

Targeted therapies represent the state-of-the-art in preclinical and clinical oncology research. The use of imatinib (Gleevec) in the treatment of chronic myelogenous leukemia (CML) serves as validation of the concept that therapeutic agents that target cancer-specific pathways can offer significant improvements over traditional chemotherapeutic agents.¹ CML is a myeloproliferative disorder that is characterized by hyperproliferation of stem cells, followed by their subsequent differentiation into peripheral white blood cells. The presence of the Philadelphia chromosome, arising from the translocation of the Abl kinase domain on chromosome 9 with a specific breakpoint cluster region (*bcr*) on chromosome 22, is characteristic of CML. The gene product of this translocation is a constitutively activated tyrosine kinase known as Bcr-Abl, which drives the proliferation of stem cells in the bone marrow and causes the resulting pathology of the disease. By targeting the tyrosine kinase activity of Bcr-Abl, imatinib normalizes peripheral white blood cell counts and substantially reduces the Philadelphia chromosome positive clone of stem cells in bone marrow, effectively offering hematological and cytogenetic responses in the clinic.

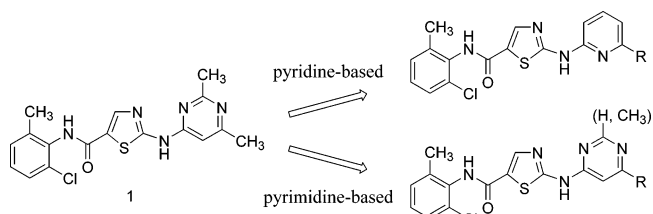
The *c*-Src proto-oncogene plays a major role in the development, growth, progression, and metastasis of a

wide variety of human cancers.² Src activation, in the form of elevated kinase activity and/or protein expression levels, has been demonstrated in several major cancer types, including colon, breast, pancreatic, lung, and brain carcinomas. Src kinase modulates signal transduction through multiple oncogenic pathways, including EGFR, Her2/neu, PDGFR, FGFR, and VEGFR. Thus, it is anticipated that blocking signaling through the inhibition of the kinase activity of Src will be an effective means of modulating aberrant pathways that drive oncologic transformation of cells.

Herein, we describe the synthesis and anticancer activity of thiazole-based dual Src/Abl kinase inhibitors. The Lck kinase activity of related 2-acylamino-5-carboxamidothiazoles has been previously described.³ Improvement in the Lck inhibitory activity of this series of compounds was afforded by replacing the 2-acyl functionality with a variety of heterocycles, leading to the identification of compound **1**.⁴ In a kinase selectivity panel, compound **1** was shown to be a potent biochemical inhibitor of multiple Src-family members, including Lck, Fyn, Src, and Hck. On the basis of the Src kinase activity of this chemical series, **1** was selected for evaluation as a potential anticancer agent.

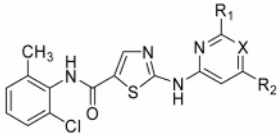
Compound **1** is a potent biochemical inhibitor of Src ($K_i = 96$ pM) and Bcr-Abl kinases ($IC_{50} < 1.0$ nM) with antiproliferative activity versus both the PC3 human prostate tumor and the K562 human blast-phase CML tumor cell lines⁵ (Table 1). This spectrum of *in vitro* activity in both a hematological and a solid tumor cell line confirmed the potential of the chemotype for oncology indications and motivated us to characterize additional analogues in an expanded panel of cellular assays including K562, PC3, MDA-MB-231 human breast tumor and WiDr human colon tumor cell lines.

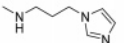
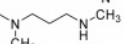
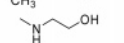
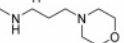
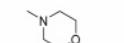
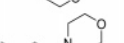
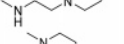
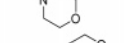
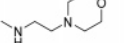
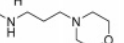
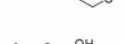
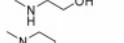
The compounds described fall into two subclasses that differ by the heterocycle appended to the 2-amino group of the thiazole. Both pyridine-based and pyrimidine-based analogues demonstrated nanomolar to sub-nanomolar inhibitory activity versus Src and Bcr-Abl and could not be effectively differentiated in biochemical assays. Thus, we focused on activity in tumor cell proliferation assays and mouse oral exposure screening to select compounds for *in vivo* evaluation in human tumor xenograft efficacy models.



The imidazolylpropylamino-substituted pyridine **2** was among the most potent compounds tested in cellular assays, demonstrating low nanomolar activity versus all four tumor types. However, at a screening dose of 50 mg/kg in the 4 h oral exposure assay, compound **2** produced low circulating plasma levels. The poor oral absorption properties of **2**, in combination with its high

* To whom correspondence should be addressed. Telephone: 609-252-4265. Fax: 609-252-7410. E-mail: louis.lombardo@bms.com.

Table 1. Antiproliferative Activities and 4 h Plasma Exposures


cmpd	X	R ₁	R ₂	cellular antiproliferative activity IC ₅₀ ^a , nM				4 hour oral exposure ^b (mouse)			PB ^c
				K562	PC3	MDA- MB-231	WiDr	AUC _{0-4h} nM*h	C _{max} nM	4 h conc nM	
1	N	CH ₃	CH ₃	1.6, 2.1	67						
2	CH		H	<3.0	2.8	<3.0	4.1	160	88	33	99
3	CH		H	<2.0	3.6 (2.1)	6.2	23	1600	780	230	
4	CH		H	<3.0	13 (8)	3.1, 5.4	7.9, 47	7200	7000	300	92
5	CH		H	<2.0	10	42, 34	32, 67	13000	8600	1100	
6	N	H		<3.0	24 (16)	45 (25)	270 (170)	1700	960	220	
7	N	H		<2.0	82	170	270	17000	9600	1900	
8	N	CH ₃		<3.0	3.6 (2.3)	16	27	160	67	37	
9	N	CH ₃		<1.0	25	47	180	3100	2200	280	
10	N	CH ₃		<2.0	14	23, 28	92, 27	11000	3100	3100	92
11	N	CH ₃		<4.0	27 (25)	140	210 (120)	1500	800	170	
12	N	CH ₃		<1.0	11 (8)	9.0 (5.1)	41	3500	2500	180	
13	N	CH ₃		<1.0	9.4 (5.6)	12 (10)	52 (38)	4800	2700	700	91

^a Antiproliferative activities were determined based on tetrazolium dye conversion following 72 h drug exposure. IC₅₀ values are reported as the mean of at least three individual determinations or as individual IC₅₀ values in the case of less than three measurements. Variability around the mean value was <50% unless otherwise indicated by an SE value in parentheses. ^b Compounds were evaluated at 50 mg/kg and formulated as solutions in 1:1 propylene glycol:water. ^c Protein binding in human serum at 10 μM compound concentration.

level of plasma protein binding, precluded further advancement to in vivo assays. Similar potent and broad spectrum cellular activity was observed with the (methylamino)propylamino- (**3**) and hydroxyethylamino- (**4**) substituted pyridines, but this encouraging profile was offset by low oral exposure (compound **3**) and apparent high clearance, as determined by the large difference between peak and 4 h plasma drug levels (compound **4**). Improvement in the pharmacokinetic profile was observed by incorporation of the morpholinopropylamine side chain in compound **5**, affording high peak plasma concentrations of 8.6 μM and sustained blood levels in excess of 1.0 μM for the duration of the 4 h assay.

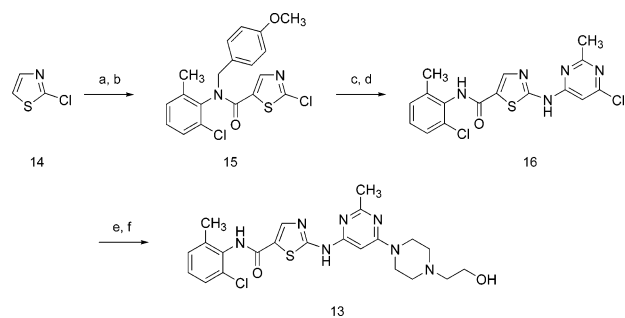
Incorporation of a variety of morpholino-tethered side chains into pyrimidine-substituted aminothiazoles met with limited success. In general, compounds **6** through **10** maintained excellent potency versus the K562 cell line, but were less effective than pyridine-substituted derivatives against solid tumor lines. Compounds **6** and **8**, bearing the morpholine directly on the pyrimidine ring, demonstrated an encouraging spectrum of cell activity, but suffered from low oral exposure in the mouse 4 h screening assay. Consistent with the favorable pharmacokinetic profile of the pyridine **5**, compounds **7** and **10** generated high and sustained blood levels following oral dosing. Conservative substitution of a methyl group on the pyrimidine ring in **9** for the hydrogen in compound **7** afforded a slight improvement

in the cellular activity profile, but had a negative impact on the compound's oral bioavailability.

To follow-up on the favorable cellular profile and reduced plasma protein binding of the pyridine **4**, the primary alcohol-substituted pyrimidines **11** through **13** were evaluated. Consistent with previous results, the hydroxyethylamino analogue **11** had excellent activity versus the K562 and PC3 cell lines. Unfortunately, the compound was substantially less effective versus the remainder of the panel.

The piperidinyl methanol **12** and piperazinyl ethanol **13** were identified as compounds with the best balance of broad spectrum antiproliferative activity and oral exposure in the mouse screening assay. Both compounds demonstrated low- to mid-nanomolar potency versus all cell lines and favorable circulating plasma levels following oral dosing. On the basis of its modest plasma protein binding and sustained blood levels for the duration of the 4 h exposure study, compound **13** was selected for characterization in additional pharmacokinetic and in vivo efficacy studies.

BMS-354825 (**13**) was prepared in 61% overall yield from the chlorothiazole **14**⁶ following an optimized synthetic sequence detailed in Scheme 1. Condensation of the lithium anion of **14** with 2-chloro-6-methylphenyl isocyanate⁷ in THF proceeded smoothly to afford the corresponding carboxamide, which was protected as the 4-methoxybenzyl derivative **15**. Displacement of the

Scheme 1. Synthesis of Compound **13**^a

^a (a) *n*-BuLi, THF, 2-chloro-6-methylphenyl isocyanate, -78°C , 86%; (b) NaH, 4-methoxybenzyl chloride, THF, 95%; (c) NaH, THF, 4-amino-6-chloro-2-methylpyrimidine, reflux, 83%; (d) TFOH, TFA/CH₂Cl₂ (1:1), 99%; (e) 1-(2-hydroxyethyl)piperazine, 1,4-dioxane, reflux; (f) HCl, Et₂O, MeOH, 91% (two steps).

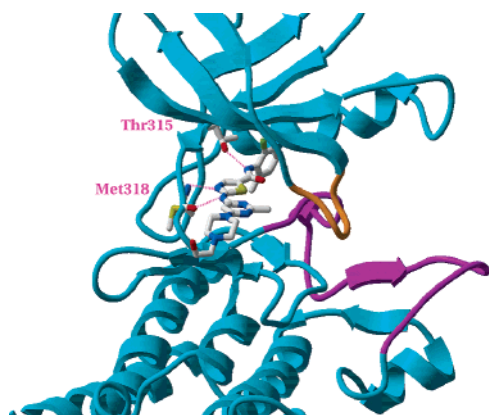


Figure 1. Ribbon diagram of the Abl kinase complex with compound **13**.

2-chloro substituent on the thiazole with the sodium salt of 4-amino-6-chloro-2-methylpyrimidine⁸ at reflux, followed by deprotection of the 4-methoxybenzyl group in TFOH/TFA gave the chloropyrimidine **16**. Finally, reaction of **16** with 1-(2-hydroxyethyl)piperazine⁹ in dioxane at reflux gave **13**, which was subsequently converted to its corresponding hydrochloride salt with methanolic HCl in ether. This sequence proved to be amenable to scale-up, and all steps were executed on 50 g or larger scale with comparable chemical yields.

A three-dimensional structure of Abl kinase complexed with **13** was determined by X-ray crystallography (Figure 1). Key features of the enzyme–inhibitor complex were identified as placement of the activation loop of Abl (depicted in magenta) in an active conformation and three hydrogen bonds between compound **13** and the protein. A pair of hydrogen bonds was formed in the hinge region of the ATP-binding site between the 2-amino hydrogen of **13** and the carbonyl oxygen of Met318 and between the 3-nitrogen of the thiazole ring of **13** and the amide nitrogen of Met318. A hydrogen bond was also formed between the hydroxyl oxygen of Thr315 and the amide nitrogen of **13**. The Abl P-loop (depicted in orange) was partially disordered, suggesting that interactions between this part of the protein and **13** were less critical for binding. It is hypothesized that these specific interactions of **13** with Abl are responsible for the compound's favorable activity versus mutant kinase forms^{10–12} (data not shown).

The Abl cocrystal structure supports and shares many of the features of a proposed binding mode for **13** with

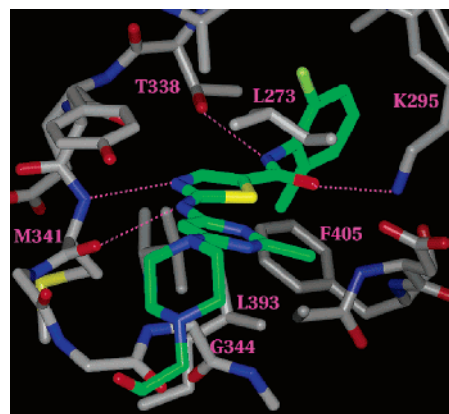


Figure 2. Compound **13** modeled into the Src kinase ATP binding site.

Table 2. Kinase Selectivity Profile of Compound **13**

kinase	enzyme IC ₅₀ , nM	kinase	enzyme IC ₅₀ , nM
Bcr-Abl	<1.0	MEK	1700
src	0.50	VEGFR-2	>2000
lck	0.40	CDK2	>5000
yes	0.50	IKK	>10000
c-kit	5.0	AKT	>50000
PDGFRβ	28	FAK	>50000
p38	100	IGF-1R	>50000
Her1	180	IR	>50000
Her2	710	MK2	>50000
FGFR-1	880	PKC α,δ,τ,ζ	>50000

Src kinase (Figure 2). The Src kinase ATP binding site was taken from PDB entry 2SRC.¹³ Compound **13** was manually docked into the ATP site and the complex was energy-minimized. All hydrogen bonds observed between Abl kinase and **13** were also observed in the Src kinase model. Additionally, a potential hydrogen bond between the amide carbonyl of **13** and Lys295 was identified. The 2-chloro-6-methylbenzamide occupies a deep hydrophobic pocket in the protein and the substituted pyrimidine occupies a hydrophobic cleft created by Leu273 and Gly344. The buried hydrophobic surface areas of both the protein and ligand in the region of the pyrimidine may account for the increased binding affinity observed in this series relative to earlier analogues.³ The pendant *N*-2-hydroxyethylpiperidine group was directed toward solvent-exposed protein and was not observed to engage in specific interactions.

To better understand the enzyme inhibitory properties of **13**, the compound was evaluated in an in-house kinase selectivity panel and *K_i* values were determined for both Src and Bcr-Abl kinase. Compound **13** was confirmed to be a highly potent, ATP competitive inhibitor of both Src and Bcr-Abl, with measured *K_i* values of 16 ± 1.0 pM and 30 ± 22 pM, respectively. The selectivity of **13** is summarized in Table 2. Consistent with the biochemical profile of **1**, compound **13** was found to potently inhibit other Src-family members. The compound also demonstrated significant activity against c-kit and PDGFRβ. Greater than 100-fold selectivity was observed for all other kinase targets in the panel.

In a rat pharmacokinetic study, **13** was characterized as having a high volume of distribution (*V_{ss}*) with systemic clearance (Cl) approximately 40% of hepatic blood flow. A 10 mg/kg oral dose administered as a solution in 1:1 propylene glycol:water was rapidly absorbed and demonstrated a favorable half-life (*t*_{1/2})

Table 3. Pharmacokinetic Properties of Compound **13** in Sprague–Dawley Rats

parameter	unit	iv dose ^a	oral dose ^a
dose	mg/kg	10	10
C_{\max}	μM	13.2 (–)	0.5 (0.2)
T_{\max}	h	–	2.2 (3.2)
AUC_{tot}	$\mu\text{M}\cdot\text{h}$	13.9 (4.6)	3.8 (2.1)
$t_{1/2}$	h	3.3 (0.9)	3.1 (0.3)
MRT	h	4.1 (1.2)	6.7 (0.6)
Cl	mL/min/mg	26.4 (7.8)	–
V_{ss}	L/kg	6.3 (2.2)	–
F_{po}	%	–	27

^a Data reported as an average of three animals with associated standard deviations in parentheses.

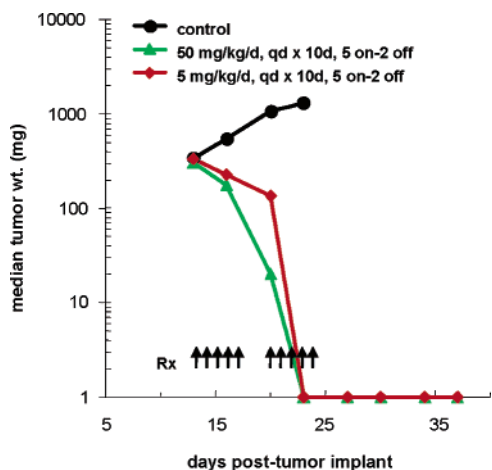


Figure 3. In vivo antitumor activity of compound **13** versus K562 xenografts in nude mice. Drug formulated as a solution in citric acid buffer at pH 4.6.

and mean residence time (MRT). The measured oral bioavailability (F_{po}) in this study was 27%. In conjunction with the mouse 4 h oral exposure data, it was concluded that **13** had a pharmacokinetic profile appropriate for continued advancement into in vivo efficacy studies. A summary of the PK parameters from the rat study is contained in Table 3.

The in vivo activity of **13** was evaluated in a K562 xenograft assay in nude mice (Figure 3). Tumor cells were implanted subcutaneously and staged to approximately 300 mg prior to two cycles of oral drug administration on a 5 day on and 2 day off schedule. Following once daily doses of either 5 or 50 mg/kg, compound **13** showed partial tumor regressions after one treatment cycle and complete disappearance of the tumor mass by the end of drug treatment. No toxicity (animal deaths, lack of weight gain) was observed in either cohort of animals. Thus, it was determined that **13** possessed potent in vivo activity and a high safety margin in this animal model of CML. The in vivo activity of **13** in imatinib-resistant¹² and imatinib-refractory models and solid tumor xenografts will be reported in separate communications.

In conclusion, a novel series of 2-(aminopyridyl)- and 2-(aminopyrimidinyl)thiazole-5-carboxamides with

potent Src and Bcr-Abl kinase inhibitory activity was identified. Analogues demonstrated broad spectrum antiproliferative activity against hematological and solid tumor cell lines originating in breast, prostate, and colon tissue. Compound **13**, a picomolar inhibitor of Src and Bcr-Abl kinase, was orally active in a K562 xenograft model of chronic myelogenous leukemia, demonstrating tumor regressions at multiple dose levels. On the basis of its favorable in vivo efficacy and pharmacokinetic profile, **13** has been advanced into clinical trials.

Acknowledgment. We thank A. Donald Crews, Christopher Ellis, Christopher Sheng, Laurence I. Wu, and Yufen Zhao for synthetic chemistry support and Bethanne Warrack and Discovery Analytical Sciences for compound characterization efforts.

Supporting Information Available: Characterization data for compounds **1** through **12**. Full experimental procedures and characterization data for compound **13**. Detailed description of pharmacokinetic assays. This material is available free of charge via the Internet at <http://pubs.acs.org>.

References

- O'Dwyer, M. E.; Mauro, M. J.; Druker, B. J. STI571 as a targeted therapy for CML. *Cancer Invest.* **2003**, *21*, 429–438.
- Frame, M. C. Src in cancer: deregulation and consequences for cell behaviour. *Biochim. Biophys. Acta* **2002**, *1602*, 114–130.
- Wityak, J.; Das, J.; Moquin, R. V.; Shen, Z.; Lin, J.; Chen, P.; Dowyeko, A. M.; Pitt, S.; Pang, S.; Shen, D. R.; Fang, Q.; De Fex, H. F.; Schieven, G. L.; Kanner, S. B.; Barrish, J. C. Discovery and initial SAR of 2-amino-5-carboxamidothiazoles as inhibitors of the Src-family kinase p56^{lck}. *Bioorg. Med. Chem. Lett.* **2003**, *13*, 4007–4010.
- Chen, P.; Norris, D.; Das, J.; Spengel, S. H.; Wityak, J.; Leith, L.; Zhao, R.; Chen, B.-C.; Pitt, S.; Pang, S.; Shen, D. R.; Zhang, R.; De Fex, H. F.; Dowyeko, A. M.; McIntyre, K. W.; Shuster, D. J.; Behnia, K.; Schieven, G. L.; Barrish, J. C. Identification of BMS-334864 as a novel, potent and orally active Src-family kinase p56^{lck} inhibitor. *Bioorg. Med. Chem. Lett.*, in press.
- Antiproliferative activities were determined based on tetrazolium dye conversion following 72 h drug exposure. Details of the assay and culture conditions for the tumor cell lines are contained in the following reference: Lee, F. Y. F.; Borzilleri, R. M.; Fairchild, C. R.; Kim, S. H.; Long, B. H.; Reventos-Suarez, C.; Vite, G. D.; Rose, W. C.; Kramer, R. A. BMS-247550: A novel epothilone analogue with a mode of action similar to paclitaxel but possessing superior antitumor efficacy. *Clin. Cancer Res.* **2001**, *7*, 1429–1437.
- Begtrup, M.; Hansen, L. B. New methods for the introduction of substituents into thiazoles. *Acta Chem. Scand.* **1992**, *46*, 372–383.
- Saito, J.; Tamura, T.; Morishima, N. JP 50,089,344, 1975.
- Ueno, K.; Kinoene, M.; Minami, T. JP 43,005,394, 1968.
- Commercially available from Sigma-Aldrich Corporation.
- Nagar, B.; Bornmann, W. G.; Pellicena, P.; Schindler, T.; Veach, D. R.; Miller, W. T.; Clarkson, B.; Kuriyan, J. Crystal structures of the kinase domain of c-Abl in complex with the small molecule inhibitors PD173955 and imatinib (STI-571). *Cancer Res.* **2002**, *62*, 4236.
- Huron, D. R.; Gorre, M. E.; Kraker, A. J.; Sawyers, C. L.; Rosen, N.; Moasser, M. M. A novel pyridopyrimidine inhibitor of Abl kinase is a picomolar inhibitor of Bcr-Abl-driven K562 cells and is effective against STI571-resistant Bcr-Abl mutants. *Clin. Cancer Res.* **2003**, *9*, 1267–1273.
- Shah, N. P.; Tran, C.; Lee, F. Y.; Chen, P.; Norris, D.; Sawyers, C. L. Overriding imatinib resistance with a novel Abl kinase inhibitor. *Science* **2004**, *305*, 399–401.
- Xu, W.; Doshi, A.; Lei, M.; Eck, M. J.; Harrison, S. C. Crystal structures of c-Src reveal features of its autoinhibitory mechanism. *Mol. Cell* **1999**, *3*, 629–638.

JM049486A